CHANSON, H. (2001). "Hydraulic Design of Stepped Spillways and Downstream Energy Dissipators." Dam Engineering, Vol. 11, No. 4, pp. 205-242 (ISSN 0 617 00563 X).

Hydraulic design of stepped spillways and downstream energy dissipators

Hubert Chanson
Reader – Fluid Mechanics, Hydraulics & Environmental Engineering
Department of Civil Engineering
The University of Queensland
Brisbane
QLD 4072
Australia
Email: h.chanson@mailbox.uq.edu.au

Abstract

Stepped channels and spillways have been used for centuries. Recently, new construction materials (eg RCC, gabions) and design techniques (eg embankment overtopping protection) have increased the interest in stepped chutes. The steps produce considerable energy dissipation along the chute and reduce the size of the required downstream energy dissipation basin. This paper reviews the hydraulic characteristics of modern stepped spillways. The basic flow patterns are described. Basic equations are developed, taking into account the free surface aeration in skimming flows. The calculations of the residual energy to be dissipated in the downstream dissipator are discussed. Simple design guidelines for the downstream energy dissipators are provided for use by professionals.

1 Introduction

Recent advances in technology have permitted the construction of large dams, reservoirs and channels [40]. This progress has necessitated the development of new design and construction techniques, particularly with the provision of adequate flood release facilities and safe dissipation of the kinetic energy of the flow. The latter may be achieved by the construction of steps on the spillway (Figures 1 and 2). A stepped chute design significantly increases the rate of energy dissipation taking

place along the spillway face, and eliminates or reduces greatly the need for a large energy dissipator at the toe of the chute.

Although the stepped cascade design was common at the end of the 19th century, much expertise has been lost since [15]. Current expertise is limited to simple geometries (ie flat horizontal steps in prismatic chutes) despite some recent interest in stepped spillway design [20, 11].

In this paper, the author first reviews the basic hydraulic characteristics of stepped channels. Then he discusses the estimate of the residual energy and provides design guidelines to size the downstream energy dissipator. The results are applied to steep stepped chutes with skimming flow that are characteristic of modern concrete spillway designs (Figures 1 and 2).

2 Hydraulics of stepped chutes: basic flow regimes

A stepped chute consists of an open channel with a series of drops in the invert. For a given chute geometry, the flow pattern may be either nappe flow at low flow rates, transition flow for intermediate discharges or skimming flow at larger flow rates (Figure 3).

At low flows (ie nappe flow regime), the total fall is divided into a number of small free-falls. The energy dissipation occurs by jet break-up in air, by jet impact on the step, and possibly with the formation of hydraulic jump on the step. The step height must be relatively large for nappe flow. This situation is not often practical but may apply to relatively flat stepped channels or at low flow rates.

For a given step geometry, an increase in flow rate may bring an intermediate flow pattern between nappe and skimming flow – the transition flow regime (Figure 3b). The transition flow is characterised by a pool of recirculating waters and often a very small air cavity, and significant spray and water deflection immediately downstream of the stagnation point. Downstream of the spray region, the supercritical flow is decelerated up to the downstream step edge. The transition flow pattern exhibits significant longitudinal variations of the flow properties on each step. It does not present the coherent appearance of skimming flows.

In a skimming flow regime, the water flows down the stepped face as a coherent stream, skimming over the steps and cushioned by the recirculating fluid trapped between them (Figures 2 and 3c). The external edges of the steps form a pseudo-bottom over which the flow skims. Beneath this, recirculating vortices develop and

are maintained through the transmission of shear stress from the water flowing past the edge of the steps. At the upstream end, the flow is smooth and no air entrainment occurs. After a few steps the flow is characterised by a strong air entrainment (Figure 2). For an observer standing on the bank, the aerated free surface has the same appearance as a self-aerated flow down a smooth invert spillway.

1.1 Prediction of the flow regime

The type of stepped flow regime is a function of the discharge and step geometry. The writer reanalysed a large number of experimental observations of changes in flow regimes. The data are summarised in Appendix I and all but one were obtained with flat horizontal steps. For each set of data, Column 6 indicates the type of transition: from nappe to transition flow (NA-TRA) or from transition to skimming flow (TRA-SK). The indication (NA-SK) suggests that the researchers ignored the transition flow regime.

Overall the results suggest that the upper limit of nappe flow may be approximated as:

$$\frac{d_c}{h} = 0.89 - 0.4 * \frac{h}{l} \qquad \text{Transition NA-TRA (1)}$$

where

d_c is the critical depth,
h is the step height, and
l is the step length,

while the lower limits of skimming flow may be estimated as:

$$\frac{d_c}{h} = 1.2 - 0.325 * \frac{h}{l} \qquad \text{Transition TRA-SK (2)}$$

Both equations are compared with the experimental data in Figure 4. Two issues must be clearly understood.

- Equations 1 and 2 were deduced for flat horizontal steps with h/l ranging from 0.05 to 1.7 (ie $3.4 < \alpha < 60°$); there is no information on their validity outside of that range and their accuracy is no better than +/-10%;
- Equations 1 and 2 characterise a change in flow regime for uniform or quasi-uniform flows only. For rapidly varied flows, the results are inaccurate. For example, at the upstream end of a stepped chute, the accelerating waters could flow as thick free-falling nappes before becoming a skimming flow regime further downstream [12].

2 Hydraulics of skimming flow

Modern concrete stepped spillways operate in a skimming flow regime (Figures 1 and 2). At the upstream end, the free surface is clear and transparent. However, a turbulent boundary layer develops along the chute invert. When the outer edge of the boundary layer reaches the free surface, free surface aeration takes place (Figure 2). The distance to the inception point of air entrainment and the flow depth at inception are best correlated by:

$$\frac{L_I}{h*\cos\alpha} = 9.719*(\sin\alpha)^{0.0796} * \left(\frac{q_w}{\sqrt{g*\sin\alpha*(h*\cos\alpha)^3}}\right)^{0.713} \quad (3)$$

$$\frac{d_I}{h*\cos\alpha} = \frac{0.4034}{(\sin\alpha)^{0.04}} * \left(\frac{q_w}{\sqrt{g*\sin\alpha*(h*\cos\alpha)^3}}\right)^{0.592} \quad (4)$$

where

L_I is the distance from the crest (measured along the invert),
D_I is the flow depth measured normal to the channel invert,
α is the chute slope,
q_w is the discharge per unit width, and
g is the gravitational constant [11] (Figure 3).

Model and prototype data are compared with Equation 3 in Figure 5. Note the good agreement between the statistical correlation and prototype data at Trigomil dam (Q_w = 1100m^3/sec). The results indicate consistently that the dimensionless distance from crest and flow depth increase with increasing dimensionless discharge (Figure 5). Further, the rate of boundary layer growth is about 2.8 times larger on stepped channels than on smooth chutes.

2.1 Rapidly varied flow at the inception point

Visual observations and detailed point measurements indicate that the flow properties are rapidly varied next to and immediately downstream of the inception point of air entrainment. Side view observations suggest that some air is entrapped in the step cavity(ies) upstream of the visual location of free-surface aeration (Figure 6).

Immediately upstream the flow is extremely turbulent and the free surface appears to be subjected to a flapping mechanism. At irregular time intervals, a water jet impinges on the horizontal step face and air is trapped in the step cavity [24, 7, 26]. An instant later, a rapid unsteady flow bulking is observed downstream (Figure 6).

Precise LDA velocity measurements by Ohtsu and Yasuda [29] indicate that, immediately upstream of the inception point, the turbulent velocity fluctuations are large, with dimensionless streamwise fluctuations u'/V of about 15-18% and normal velocity fluctuations v'/V of about 2-4%, where u' and v' are the root mean square of longitudinal and lateral components of turbulent velocity, respectively (Figure 6c). In Figure 6c, observed values of $v' \approx 0.14$m/sec next to the free surface are large enough to initiate air bubble entrainment [10].

Immediately downstream of the inception point, time-averaged air concentration data show a sudden aeration. For example, an increase in mean air concentration ΔC_{mean} = 25% along a distance $\Delta s = 6.5 * d_c$ down a 30° slope for d_c/h = 5.2 [5]; an increase in mean air concentration ΔC_{mean} = 55% in 18 step heights down a 53° slope for $d_c/h \leq 2$ [26]; an increase in mean air concentration ΔC_{mean} = 32% in 2 step heights down a 22° slope for d_c/h = 1.1, where C_{mean} is the mean air concentration.

2.2 Gradually varied flow properties

Downstream of the inception point, the flow is fully developed and the flow properties tend gradually to uniform equilibrium (ie normal flow conditions). While the flow resistance on smooth invert chutes is primarily skin friction, skimming flows over stepped chute are characterised by significant form losses. The water skims over the step edges with formation of recirculating vortices between the main stream and the step corners. Form drag is predominant. The reanalysis of over 650 laboratory and prototype data showed that the dimensionless friction coefficient f (or Darcy friction factor) is about 0.1-0.3, with an analytical development implying f = 0.2 [14]. The results are independent of the step height within limits ($1 \leq d_c/h \leq 10$).

On smooth invert chutes, the gradually varied flow properties are deduced from the differential form of the energy equation or backwater equation:

$$\frac{\partial H}{\partial s} = -S_f \tag{5}$$

where

H is the mean total head,
S_f is the friction slope, and
S is the longitudinal coordinate in the flow direction.

In stepped chute flows, several researchers, including the writer, have attempted unsuccessfully to apply the backwater equation (Equation 5) based on the Darcy-Weisbach friction factor and without introducing "fudging" coefficients.

It is believed that two basic assumptions of the backwater calculations are violated in skimming flows. These are (a) the flow must be gradually varied and (b) the flow resistance must be the same as for a uniform flow [17,14]. The form drag and associated cavity recirculation are very energetic processes and the flow properties in the mixing layer are rapidly varied. A number of researchers showed drastic differences between void fraction and velocity data measured at the step edge and above the cavity at one step, as well as from one step to the adjacent ones [29, 27]. The concept of gradual variation of the flow resistance is inappropriate in a form

drag-dominated skimming flow. (Indeed Equation 5 assumes a one-dimensional flow motion that is untrue.)

2.3 Free surface aeration

In the fully developed flow region, free surface aeration is significant. Turbulence acting next to the free surface is large enough to overcome both surface tension for the entrainment of air bubbles and buoyancy to carry the bubbles downward. The diffusion of air bubbles may be approximated by a simple analytical model:

$$C = 1 - \tanh^2\left(K' - \frac{y}{2 * D' * Y_{90}}\right) \quad (6)$$

where

C	is the void fraction (or air concentration),
tanh	is the hyperbolic tangent function,
y	is the distance normal to the pseudo-invert formed by the step edges,
Y_{90}	is the distance where C = 90%,
D'	is a dimensionless turbulent diffusivity,
K'	is an integration constant, and
D' and K'	are functions of the mean air content C_{mean} only (Table 1), where C_{mean} is the depth averaged air content defined in terms of Y_{90}:

$$C_{mean} = \frac{1}{Y_{90}} * \int_0^{Y_{90}} C * dy \quad (7)$$

Equation 6 was tested successfully with stepped chute data obtained in models and prototype (Figure 7) although it was originally developed for smooth invert chute flows [13].

In the gradually varied flow region, experimental data show a gradual increase in mean air content along the chute (Figure 8). For a channel of constant width and channel slope, the analytical solution of the continuity equation for air yields:

$$\frac{1}{(1-C_e)^2} * Ln\left(\frac{1-C_{mean}}{C_e - C_{mean}}\right) - \frac{1}{(1-C_e)*(1-C_{mean})} = k_o * s' + K_o \quad (8)$$

where K_o and k_o are:

$$k_o = \frac{u_r * d_I * \cos\alpha}{q_w}$$

$$K_o = \frac{1}{1-C_e} * \left(\frac{1}{1-C_e} * Ln\left(\frac{1-C^*}{C_e - C^*}\right) - \frac{1}{1-C^*}\right)$$

d_I is the flow depth at the inception point ($s = L_I$), $s' = (s - L_I)/d_I$,

s is the longitudinal coordinate in the invert, and

C^* is the mean air concentration at the reference location ($s = L_I$) [42, 10].

The uniform equilibrium mean air content C_e is a function of the slope α only. For slopes less than 50°, it may be estimated as: $C_e = 0.9*\sin\alpha$.

Equation 8 allows the calculations of the average air concentration C_{mean} as a function of the distance along the chute independently of the velocity, roughness and flow depth. Results are compared with experimental data in Figure 8. The calculations were performed with u_r = 0.4m/sec and C^* = 0.2. The former value is characteristic of millimetric size bubbles and it was used for the Aviemore dam spillway modelling [10].

Experimental works by Boes [5], and Matos [26], suggest that a reasonable approximation is C^* = 0.2 at the inception point: ie to take into account the sudden flow aeration in the rapidly varied flow immediately downstream of the inception point.

3 Residual energy downstream of stepped chutes

Design engineers need to predict accurately the downstream kinetic energy of the flow to size the energy dissipator. At the downstream end of the chute, the residual head equals:

$$H_{res} = d * \cos\alpha + \frac{q_w^{\,2}}{2 * g * d^2} \quad (9)$$

where d is the clear water depth:

$$d = \int_0^{Y90} (1 - C) * dy \quad (10)$$

For steep chutes ($\alpha \sim 35$ to $55°$), both the flow acceleration and boundary layer development affect the flow properties significantly. The complete flow calculations can be tedious and backwater calculations are not suitable (see above). Complete calculations of developing flow and uniform equilibrium flow may be combined to provide a general trend which may be used for a preliminary design (Figure 9).

Ideally, the maximum velocity at the downstream chute end is:

$$V_{max} = \sqrt{2 * g * (H_{max} - d * \cos\alpha)} \quad (11)$$

where

H_{max} is the upstream total head,
d is the ideal flow depth ($d = q_w/V_{max}$), and
V_{max} is the ideal fluid flow velocity (Figure 9a).

In practice the downstream flow velocity U_w is smaller than the theoretical velocity V_{max} because of friction losses.

In Figure 9, the mean flow velocity is plotted as U_w/V_{max} versus H_{max}/d_c where V_{max} is the theoretical velocity (Equation 11), H_{max} is the upstream total head and d_c is the critical depth. Both developing flow calculations and uniform equilibrium flow calculations are shown. Fitting curves are plotted to connect these lines (Figure 9b).

Experimental data based upon air concentration distribution measurements are compared with theoretical calculations in the developing flow region and in the uniform equilibrium flow region. The curves are valid for skimming flow with slopes ranging from 35 to 55° (ie 1V:2.1H to 1V:0.7H).

The stepped chute data and calculations are also compared with smooth chute calculations [14]. Larger energy dissipation takes place along a stepped spillway, compared with a smooth chute, and the size of the downstream stilling basin can be reduced with a stepped chute.

4 Design of the energy dissipator

The residual energy is to be dissipated in a downstream energy dissipator.

Energy dissipation on dam spillways is achieved usually by a standard stilling basin, in which a hydraulic jump is created to dissipate a large amount of flow energy and to convert the flow from supercritical to subcritical conditions, a high velocity water jet taking off from a flip bucket and impinging into a downstream plunge pool, or a plunging jet pool in which the spillway flow impinges and the kinetic energy is dissipated in turbulent recirculation. The stilling basin is the common type of dissipators for weirs and small dams. Most energy is dissipated in a hydraulic jump assisted by appurtenances (eg step, baffle blocks) to increase the turbulence. The energy dissipator must be designed to operate safely for a wide range of flow rates and tailwater flow conditions.

The basic steps in the spillway design procedure are: selecting the crest elevation and width; determining the design discharge Q_w from risk analysis and flood routing; calculating the upstream head above spillway crest for the design flow rate; and choosing the apron elevation.

For the design flow conditions, the flow properties at the chute toe may be estimated using Figure 9. Figure 9 provides an estimate of the flow velocity U_w, the clear-water flow depth $d = q_w/U_w$ and the residual energy (Equation 9) as a function of the maximum head above chute toe and flow rate. For a hydraulic jump stilling

basin, the conjugate (subcritical) flow conditions are deduced from the momentum equation and the roller length may be calculated from empirical correlations [23]. The apron length must be greater than the jump length. Then the jump height rating level must be compared with the tailwater rating level. If the jump height rating level does not match the tailwater rating level, the hydraulic jump will not take place on the apron.

4.1 Design application: Riou dam

A simple design application is the Riou dam (Figure 1).

Completed in 1990, the dam is a 22m high RCC gravity structure. The overflow stepped spillway is designed to pass 110m^3/sec. It consists of a broad crest (W = 96m) followed by a straight chute with 42 steps (h = 0.43m, l = 0.72m) and a 5m long stilling basin.

At design flow conditions, Figure 3 indicates that the spillway operates in a skimming flow regime. The point of free surface aeration inception is located about 11 step heights downstream of the crest (Equation 3). At the downstream end of the chute, the mean air content will be about 0.5 (Equation 8). Figure 9 predicts U_w = 7.1m/sec and d = 0.16m at the downstream end of the chute. For the corresponding Froude number, the head loss in the hydraulic jump is 54% of the residual head at the downstream end of the chute (H_{res} = 2.7m) and the roller length is about 5.2m. This result is consistent with the size of the stilling basin.

For the same structure equipped with a smooth-invert chute (α = 59°), the flow properties at the downstream end of the chute would be: U_w = 13.2m/sec, H_{res} = 9m and the Froude number 14.4. This value corresponds to a strong hydraulic jump associated with large invert pressure fluctuations and high risks of bed erosion.

In summary, the selection of a stepped chute at the Riou dam provides a means to reduce the size and cost of the downstream stilling basin. At design flow, 85% of the total head loss is dissipated on the stepped chute and the residual head is dissipated in the stilling basin.

5 Conclusion

The recent interest in stepped chutes has been associated with the development of new construction material and design techniques. The steps increase significantly the

rate of energy dissipation taking place along the chute and reduce the size of the required downstream energy dissipation basin.

For a given chute geometry and flow rate per unit width, the flow regime may be either a nappe flow, transition or skimming flow (Figure 3). Experimental observations are summarised in Figure 4 and Appendix I. Modern stepped spillways are characterised by a steep slope and large flow rates for which the waters spill as a skimming flow. On the upper steps, the free surface is smooth and glassy, and no free-surface aeration is observed. Turbulence is however generated by the stepped invert and a turbulent boundary layer develops until the outer edge reaches the free surface. That location, called the inception point of air entrainment, is characterised by sudden flow aeration and by rapidly varied flow properties. Downstream the fully developed flow is aerated and the flow characteristics vary gradually. Free surface aeration may be calculated using Equations 6 and 8. The clear water flow velocity U_w cannot be computed with "traditional" equations but it may be estimated using a graphical method (Figure 9). With the knowledge of the air-water flow properties, the downstream energy dissipator may be designed more accurately. An example is developed for the Riou dam (Figure 1).

Despite an increased knowledge of stepped channel flows, there is a lack of expertise and knowledge on the hydraulic characteristics of skimming flows past flat slopes, the hydraulics of the transition flow regime, the mechanisms of flow recirculation in skimming flow regime, and the air-water gas transfer process in the nappe and skimming flow regimes. Furthermore, the present paper has characterised the hydraulics of skimming flow for prismatic rectangular channels with flat horizontal steps. Little information is available for non-rectangular channels and three-dimensional flows.

Acknowledgements

The writer acknowledges the helpful assistance of the following people (in alphabetical order): Dr R Baker (University of Salsford, UK), John Laboon (US Bureau of Reclamation), Dr J Matos (IST, Portugal), Dr A N Pinheiro (IST, Portugal), Professor I Ohtsu (Nihon University, Japan), Dr J L Sanchez-Bribiesca and F Gonzalez-Villareal (UNAM, Mexico), Dr L Toombes (University of Queensland, Australia), Dr Y Yasuda (Nihon University, Japan).

Notation

C air concentration defined as the volume of air per unit volume (NB: it is also called void fraction);

C_e equilibrium depth averaged air concentration for uniform equilibrium flow;

C_{mean} depth averaged air concentration defined as: $(1 - Y_{90}) * C_{mean} = d$;

C^* integration constant characteristic of the rapid free surface aeration next to the inception point;

D' dimensionless air bubble diffusivity (defined by [13]);

d equivalent clear-water flow depth (m) defined as: $d = \int_0^{Y_{90}} (1 - C) * dy$;

d_I flow depth at the inception point (m);

d_c critical flow depth (m); for a rectangular channel: $d_c = \sqrt[3]{q_w^{\,2} / g}$;

d_t step pool height (m);

F^* Froude number defined in terms of the step roughness height: $F^* = q_w / \sqrt{g * \sin\alpha * (h * \cos\alpha^3)}$;

f Darcy friction factor;

g gravity constant (m^2/sec), or acceleration of gravity;

H total head (m);

H_{dam} dam height (m): ie dam crest head above downstream toe;

H_{max} maximum head available (m) using the spillway toe as datum;

H_{res} residual head (m) at the dowsntream end of the spillway chute, using the spillway toe as datum;

h height of steps (m) (measured vertically);

K_o integration constant;

K' integration constant (defined by [13]);

k_o integration constant;

L_I distance from the start of growth of boundary layer to the inception point of air entrainment;

l horizontal length of steps (m) (measured perpendicular to the vertical direction);

Q_w water discharge (m^3/sec);

q_w water discharge per unit width (m^2/sec);

S_f friction slope;

s curvilinear coordinate (m): ie distance measured along the channel bottom;

s' dimensionless curvilinear coordinate : $s' = (s - L_I)/d_I$,

U_w clear-water flow velocity (m/sec): $U_w = q_w/d$;

u' root mean square of longitudinal component of turbulent velocity (m/sec);

u_r rise bubble velocity (m/sec);

V local velocity (m/sec);

V_{max} ideal fluid velocity (m/sec) at the chute toe;

v' root mean square of lateral component of turbulent velocity (m/sec);

W channel width (m);

Y_{90} characteristic depth (m) where the air concentration is 90%;

α channel slope.

Subscript

I inception point of free surface aeration;

w water flow.

References

1 BaCaRa, "Etude de la dissipation d'energie sur les evacuateurs à marches", ('Study of the energy dissipation on stepped spillways'), *Rapport d'Essais*, Projet National BaCaRa, CEMAGREF-SCP, Aix-en-Provence, France, 111 pages (in French), October 1991

2 Baker R, "Brushes clough wedge block spillway - Progress Report No 3", *SCEL Project Report No SJ542-4*, University of Salford, UK, 47 pages, November 1994

3 Beitz E & Lawless M, "Hydraulic model study for dam on GHFL 3791 Isaac River at Burton Gorge", *Water Resources Commission Report*, Ref No REP/24.1, Brisbane, Australia, September 1992

4 Bindo M, Gautier J & Lacroix F, "The stepped spillway of M'Bali dam", *International Water Power & Dam Construction*, Vol 45, No 1, pp35-36, 1993

5 Boes R M, "Physical model study on two-phase cascade flow", *Proc 28th IAHR Congress*, Graz, Austria, Session S1, 6 pages (CD-ROM), 1991

6 Boes R M, "Zweiphasenstroömung und energieumsetzung auf grosskaskaden", ('Two-phase flow and energy dissipation on cascades'), *PhD Thesis*, VAW-ETH, Zürich, Switzerland (in German), 2000

7 Chamani M R, "Air inception in skimming flow regime over stepped spillways", *Intl Workshop on Hydraulics of Stepped Spillways*, Zürich, Switzerland, H E Minor & W H Hager, Editors, Balkema Publ, pp61-67, 2000

8 Chamani M R & Rajaratnam N, "Onset of skimming flow on stepped spillways", *Jl of Hyd Engrg*, ASCE, Vol 125, No 9, pp969-971, 1999b

9 Chamani M R & Rajaratnam N, "Characteristics of skimming flow over stepped spillways", *Jl of Hyd Engrg*, ASCE, Vol 125, No 4, pp361-368, 1999a

10 Chanson H, "Self-aerated flows on chutes and spillways" *Jl of Hyd Engrg*, ASCE, Vol 119, No 2, pp220-243. Discussion: Vol 120, No 6, pp778-782, 1993

11 Chanson H, "Hydraulic design of stepped cascades, channels, weirs and spillways", *Pergamon*, Oxford, UK, 292 pages, January 1995

12 Chanson H, "Prediction of the transition nappe/skimming flow on a stepped channel", *Jl of Hyd Res*, IAHR, Vol 34, No 3, pp421-429, 1996

13 Chanson H, "Air bubble entrainment in free surface turbulent shear flows", *Academic Press*, London, UK, 401 pages, 1997
14 Chanson H, "The hydraulics of open channel flows: an introduction", *Edward Arnold*, London, UK, 512 pages, 1999
15 Chanson H, "Forum article. Hydraulics of stepped spillways: current status", *Jl of Hyd Engrg*, ASCE, Vol 126, No 9, 2000
16 Chanson H, Yasuda Y & Ohtsu I, "Flow resistance in skimming flow: a critical review", *Intl Workshop on Hydraulics of Stepped Spillways*, Zürich, Switzerland, H E Minor & W H Hager, Editors, Balkema Publ, pp95-102, 2000
17 Chow V T, "Open channel hydraulics", *McGraw-Hill*, New York, USA, 1959
18 DNR, Private Communication, 1989
19 Elviro V & Mateos C, "Spanish research into stepped spillways", *Intl Jl Hydropower & Dams*, Vol 2, No 5, pp61-65, 1995
20 Essery I T S & Horner M W, "The hydraulic design of stepped spillways", *CIRIA Report No 33*, 2nd Edition, London, UK, January 1978
21 Frizell K H & Mefford B W, "Designing spillways to prevent cavitation damage", *Concrete International*, Vol 13, No 5, pp58-64, 1991
22 Haddad A A, "Water flow over stepped spillway", *Masters Thesis*, Polytechnic of Bari, Italy, 1998
23 Hager W H, Bremen R & Kawagoshi N, "Classical hydraulic jump: length of roller", *Jl of Hyd Res*, IAHR, Vol 28, No 5, pp591-608, 1990
24 Horner M W, "An analysis of flow on cascades of steps", *PhD Thesis*, Univ of Birmingham, UK, 1969
25 Kells J A, "Comparison of energy dissipation between nappe and skimming flow regimes on stepped chutes – discussion", *Jl of Hyd Res*, IAHR, Vol 33, No 1, pp128-133, 1995
26 Matos J, "Hydraulic design of stepped spillways over RCC dams," *Intl Workshop on Hydraulics of Stepped Spillways*, Zürich, Switzerland, H E Minor & W H Hager, Editors, Balkema Publ, pp187-194, 2000
27 Matos J, Sanchez M, Quintela A & Dolz J, "Characteristic depth and pressure profiles in skimming flow over stepped spillways", *Proc 28th IAHR Congress*, Graz, Austria, Session B14, 6 pages (CD-ROM), 1999
28 Montes J S, Private Communication (in Chanson 1996), 1994

29 Ohtsu I & Yasuda Y, "Characteristics of flow conditions on stepped channels", *Proc 27th IAHR Biennal Congress*, San Francisco, USA, Theme D, pp583-588, 1997

30 Peyras L, Royet P & Degoutte G, "Ecoulement et dissipation sur les déversoirs en gradins de gabions", ('Flows and dissipation of energy on gabion weirs'), *Jl La Houille Blanche*, No 1, pp37-47 (in French), 1991

31 Pinheiro A N & Fael C S, "Nappe flow in stepped channels – occurrence and energy dissipation", *Intl Workshop on Hydraulics of Stepped Spillways*, Zürich, Switzerland, H E Minor & W H Hager, Editors, Balkema Publ, pp119-126, 2000

32 Ru S X, Tang C Y, Pan R W & He X M, "Stepped dissipator on spillway face", *Proc 9th APD-IAHR Congress*, Singapore, Vol 2, pp193-200, 1994

33 Ruff J F & Frizell K H "Air concentration measurements in highly-turbulent flow on a steeply-sloping chute", *Proc Hydraulic Engineering Conf*, ASCE, Buffalo, USA, Vol 2, pp999-1003, 1994

34 Sanchez-Bribiesca J L & Gonzalez-Villareal F, "Spilling floods cost effectively", *International Water Power & Dam Construction*, Vol 48, No 5, pp16-20, 1996

35 Shvainshtein A M, "Stepped spillways and energy dissipation", *Gidrotekhnicheskoe Stroitel'stvo*, No 5, pp15-21 (in Russian), 1999. (Also Hydrotechnical Construction, Vol 3, No 5, 1999, pp275-282)

36 Sorensen R M, "Stepped spillway hydraulic model investigation", *Jl of Hyd Engrg*, ASCE, Vol 111, No 12, pp1461-1472. Discussion: Vol 113, No 8, pp 1095-1097, 1985

37 Stephenson D, "Stepped energy dissipators", *Proc Intl Symp on Hydraulics for High Dams*, IAHR, Beijing, China, pp1228-1235, 1988

38 Tozzi M J, "Caracterização/comportamento de escoamentos em vertedouros com paramento em degraus", ('Hydraulics of stepped spillways'), *PhD Thesis*, University of São Paulo, Brazil (in Portuguese), 1992

39 Tozzi M, Taniguchi E & Ota J, "Air concentration in flows over stepped spillways", *Proc 1998 ASME Fluids Eng Conf*, FEDSM'98, Washington DC, USA, Paper FEDSM98-5053, 7 pages (CD-ROM), 21-25 June, 1998

40 Vischer D & Hager W H, "Dam hydraulics", *John Wiley*, Chichester, UK, 316 pages, 1998

41 Wahrheit-Lensing A, "Selbstbeluftung und energieumwandlung beim anfluss uber treppenformige entlastungsanlagen", ('Self-aeration and energy dissipation in flow over stepped spillways'), *PhD Thesis*, Karlsruhe University, Germany, 164 pages (in German), 1996

42 Wood I R, "Air water flows", *Proc 21st IAHR Congress*, Melbourne, Australia, Keynote address, pp18-29, 1985

43 Yasuda Y & Ohtsu I, "Flow resistance of skimming flow in stepped channels", *Proc 28th IAHR Congress*, Graz, Austria, Session B14, 6 pages (CD-ROM), 1999

44 Zhou Hui, "Hydraulic performances of skimming flow over stepped spillway", *Proc 10th APD-IAHR Congress*, Langkawi Island, Malaysia, pp1-8, August 1996

Ref (1)	Slope α (deg) (2)	$\frac{h}{l}$ (3)	Step height h (m) (4)	$\frac{d_c}{h}$ Onset (5)	Type of transition (6)	Remarks (7)
Horner (1969)	22.8	0.42	0.029	0.81	NA-SK	30-step model.
	27.8	0.53	0.036	0.8	NA-SK	Horiz steps.
	36.4	0.74	0.051	0.82	NA-SK	Fig 4.16
	40.4	0.85	0.069	0.79	NA-SK	
Essey & Horner (1978)	11.3	0.2	0.05	1.15	NA-SK	Flat horizontal steps
	22.8	0.42	0.029	0.81	NA-SK	
	27.7	0.53	0.036	0.82	NA-SK	
	36.4	0.74	0.05	0.82	NA-SK	
	40.1	0.84	0.057	0.8	NA-SK	
Peyras *et al* (1991)	18.4	0.33	0.2	0.74	NA-SK	Gabion. Flat horizontal steps
	26.6	0.5	0.2	0.67	NA-SK	
	45	1	0.2	0.61	NA-SK	
Beitz & Lawless (1992)	51.3	1.25	0.02	0.4	NA-SK	Flat horizontal steps
DNR (1989)	18.4	0.33	0.067	0.56	NA-SK	Pooled steps: $d_t/h = 0.1$
Montes (1994)	45	1	-	0.62	NA-SK	Flat horizontal steps
	36.9	0.75	-	0.9	NA-SK	
Kells (1995)	45	1	-	0.5	NA-SK	Gabions: horizontal capped (impervious) steps
Stephenson (1988)	45	1	7.543	0.74	NA-SK	Flat horizontal steps
	26.6	0.5	5.996	0.77	NA-SK	
	18.4	0.33	4.871	0.79	NA-SK	
	11.3	0.2	3.609	0.83	NA-SK	
Elviro & Mateos (1995)	53.1	1.33	-	0.51	NA-TRA	
	53.1	1.33	-	0.72	TRA-SK	
Ru *et al* (1994)	53.1	1.33	0.08	0.57	NA-SK	Model E (or B4). Flat horizontal steps ▶

Appendix I. Experimental data: transition flow conditions (*cont on pp224-225*)

Ref (1)	Slope α (deg) (2)	$\frac{h}{l}$ (3)	Step height h (m) (4)	$\frac{d_c}{h}$ Onset (5)	Type of transition (6)	Remarks (7)
Ohtsu & Yasuda (1997)	-	0.35	-	1.08	TRA-SK	Flat horizontal steps. Lower limit of skimming flow
	-	0.58	-	0.95	TRA-SK	
	-	1	-	0.83	TRA-SK	
	-	1.44	-	0.8	TRA-SK	
	-	0.35	-	0.79	NA-TRA	Upper limit of nappe flow
	-	0.58	-	0.77	NA-TRA	
	-	1	-	0.6	NA-TRA	
Haddad (1998)	25.6	0.48	0.024	0.98	TRA	Flat horizontal steps. Transition
	13.5	0.24	0.024	1.37	NA-TRA	Upper limit of nappe flow
	13.5	0.24	0.024	1.46	TRA-SK	Lower limit of skimming flow
	6.8	0.12	0.024	0.88	NA-TRA	W = 0.75m
	6.8	0.12	0.024	1.15	TRA-SK	
	13.5	0.24	0.024	0.88	NA-TRA	
	13.5	0.24	0.024	1.11	TRA-SK	
	25.6	0.48	0.024	0.72	NA-TRA	
	25.6	0.48	0.024	0.98	TRA-SK	
Chamani & Rajaratnam (1999)	59.1	1.67	-	0.26	NA-TRA	Flat horizontal steps. h = 0.125, 0.0625, 0.0312m
	59.1	1.67	-	0.22	NA-TRA	
	59.1	1.67	-	0.2	NA-TRA	
	51.3	1.25	-	0.36	NA-TRA	h = 0.125 & 0.03125m
	51.3	1.25	-	0.32	NA-TRA	
Pinheiro & Fael (2000)	18.4	0.33	0.05	0.95	NA-SK	Flat horizontal steps. W = 0.7m
	14	0.25	0.05	1.16	NA-SK	
Shvainshtein (1999)	38.7	0.8	0.05	0.72	NA-SK	W = 0.48m
	51.3	1.25	0.0625	0.72	NA-SK	Flat horizontal steps
Boes (2000)	30	0.58	-	0.83	NA-SK	Supercritical inflow
	50	1.19	-	0.74	NA-SK	Flat horizontal steps

Appendix I. Experimental data: transition flow conditions

Ref (1)	Slope α (deg) (2)	$\frac{h}{l}$ (3)	Step height h (m) (4)	$\frac{d_c}{h}$ Onset (5)	Type of transition (6)	Remarks (7)
Present study	3.4	0.06	-	1.07	NA-TRA	Supercritical inflow. Flat horizontal steps. h = 0.143 & 0.07m. W = 0.5m
	22	0.4	0.1	0.53	NA-TRA	Broad-crest. Flat horizontal steps. h = 0.10m. W = 1m
	22	0.4	0.1	0.97	TRA-SK	

Notes

Type of transition:

NA-SK = from nappe to skimming flow;

NA-TRA = from nappe to transition flow;

TRA-SK = from transition to skimming flow;

TRA = transition flow conditions.

Data re-analysis by the author.

Appendix I. Experimental data: transition flow conditions

C_{mean} (1)	D' (2)	K' (3)
0.01	0.007312	68.70445
0.05	0.036562	14.0029
0.1	0.073124	7.16516
0.15	0.109704	4.88517
0.2	0.146489	3.74068
0.3	0.223191	2.567688
0.4	0.3111	1.93465
0.5	0.423441	1.508251
0.6	0.587217	1.178924
0.7	0.878462	0.896627

Table 1. Relationship between C_{mean}, D' and K' (after [13])

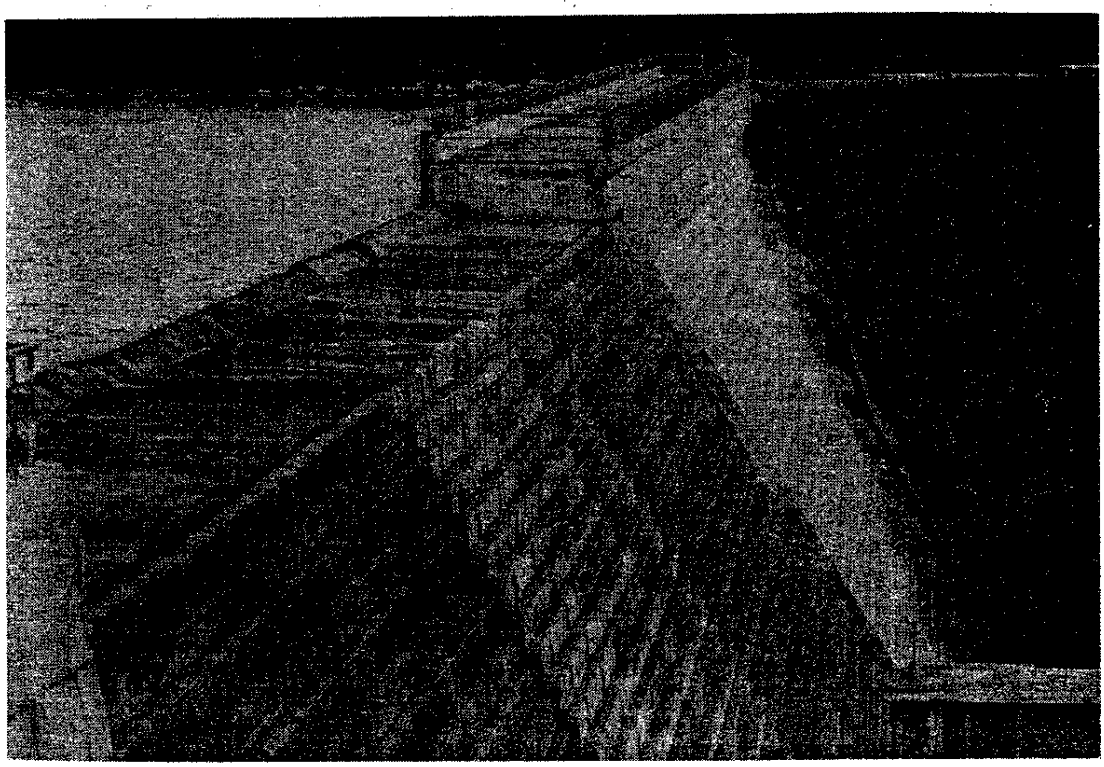

Figure 1. Riou dam, France (1990) – H_{dam} = 22m, RCC gravity dam with overflow stepped spillway (design flow: 110m³/sec, h = 0.43m, α = 59°)
(a) view from the right bank (note the broad crest design)

Figure 1. Riou dam, France (1990) – H_{dam} = 22m, RCC gravity dam with overflow stepped spillway (design flow: 110m³/sec, h = 0.43m, α = 59°)
(b) view from the downstream in 1998 (note the short stilling basin)

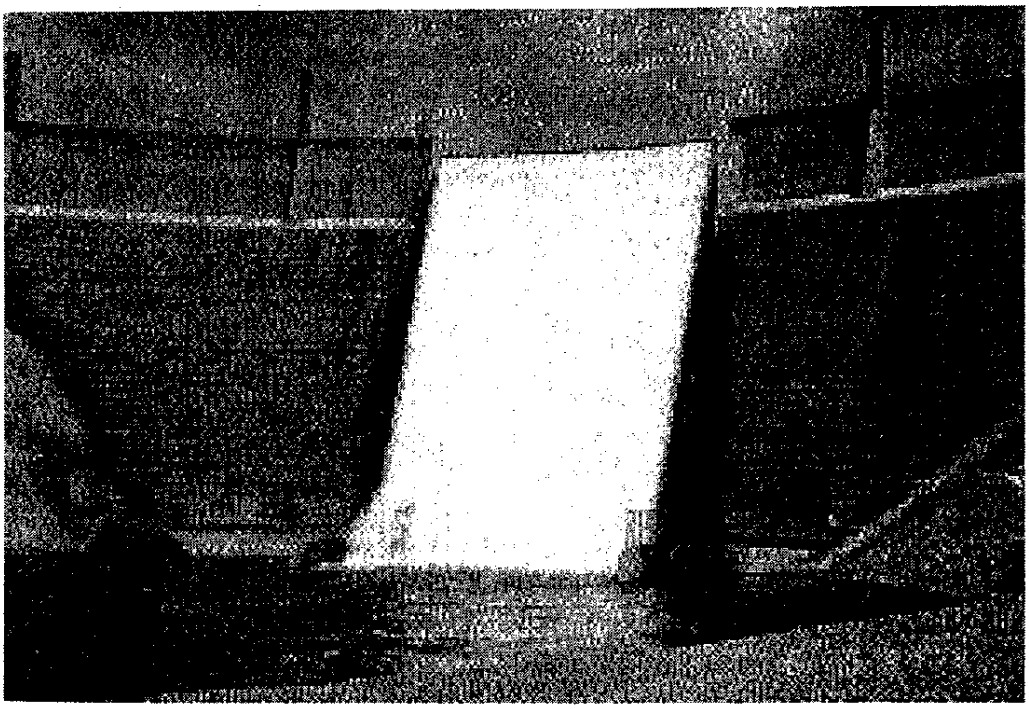

Figure 2. Santa Cruz dam, New Mexico, USA, in 1991 – H_{dam} = 46m, 1929 concrete arch dam reinforced by RCC and conventional concrete buttresses in 1987, with a new stepped spillway (design flow: 56.3m³/sec)

(Courtesy of the US Bureau of Reclamation)

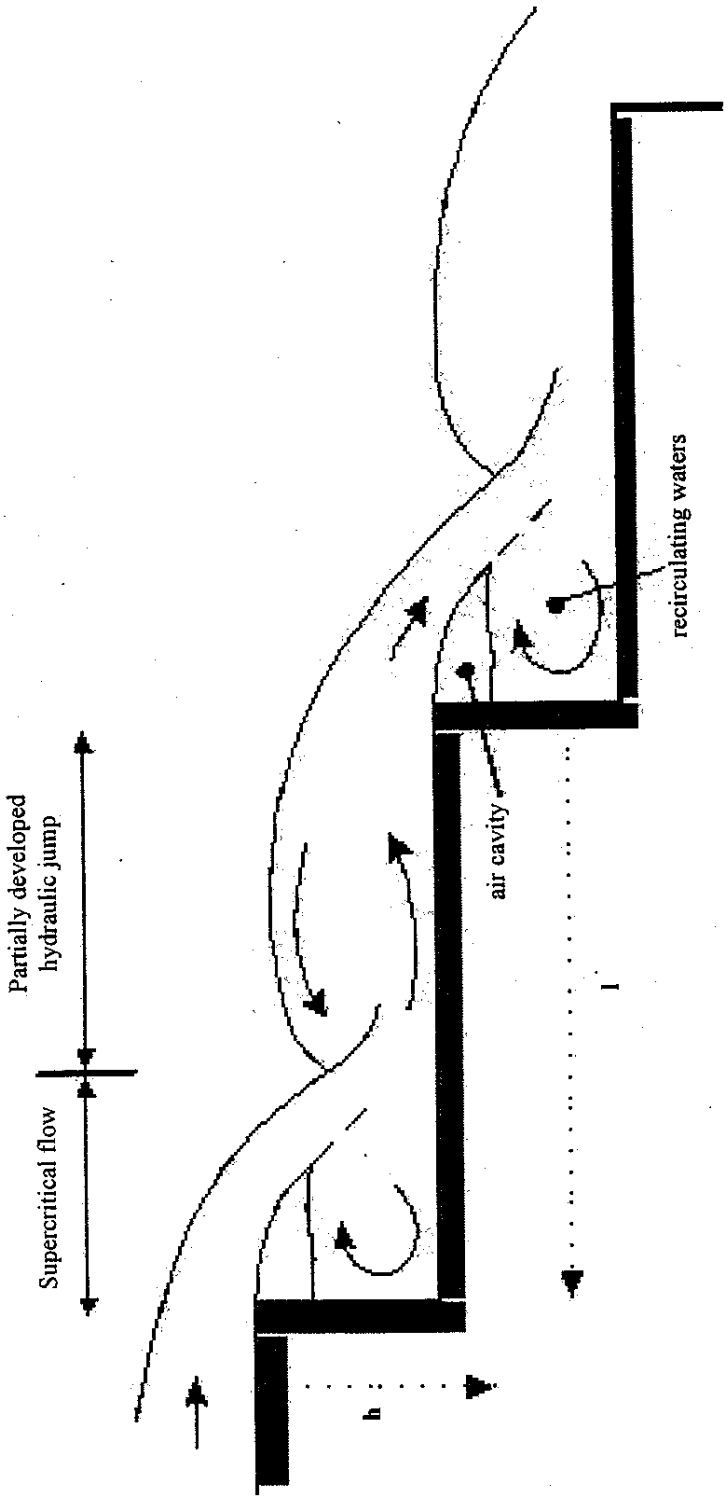

Figure 3. Basic flow regimes above a stepped chute
(a) Nappe flow regime with hydraulic jump

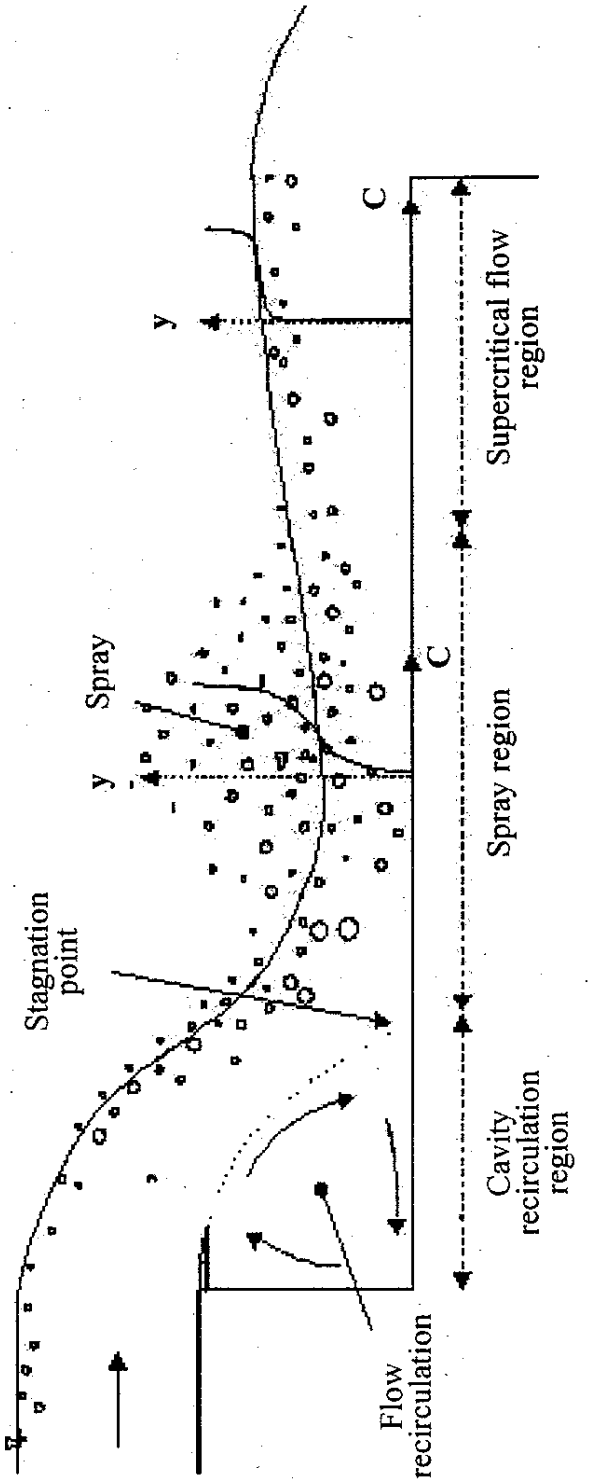

Figure 3. Basic flow regimes above a stepped chute
(b) A form of transition flow regime

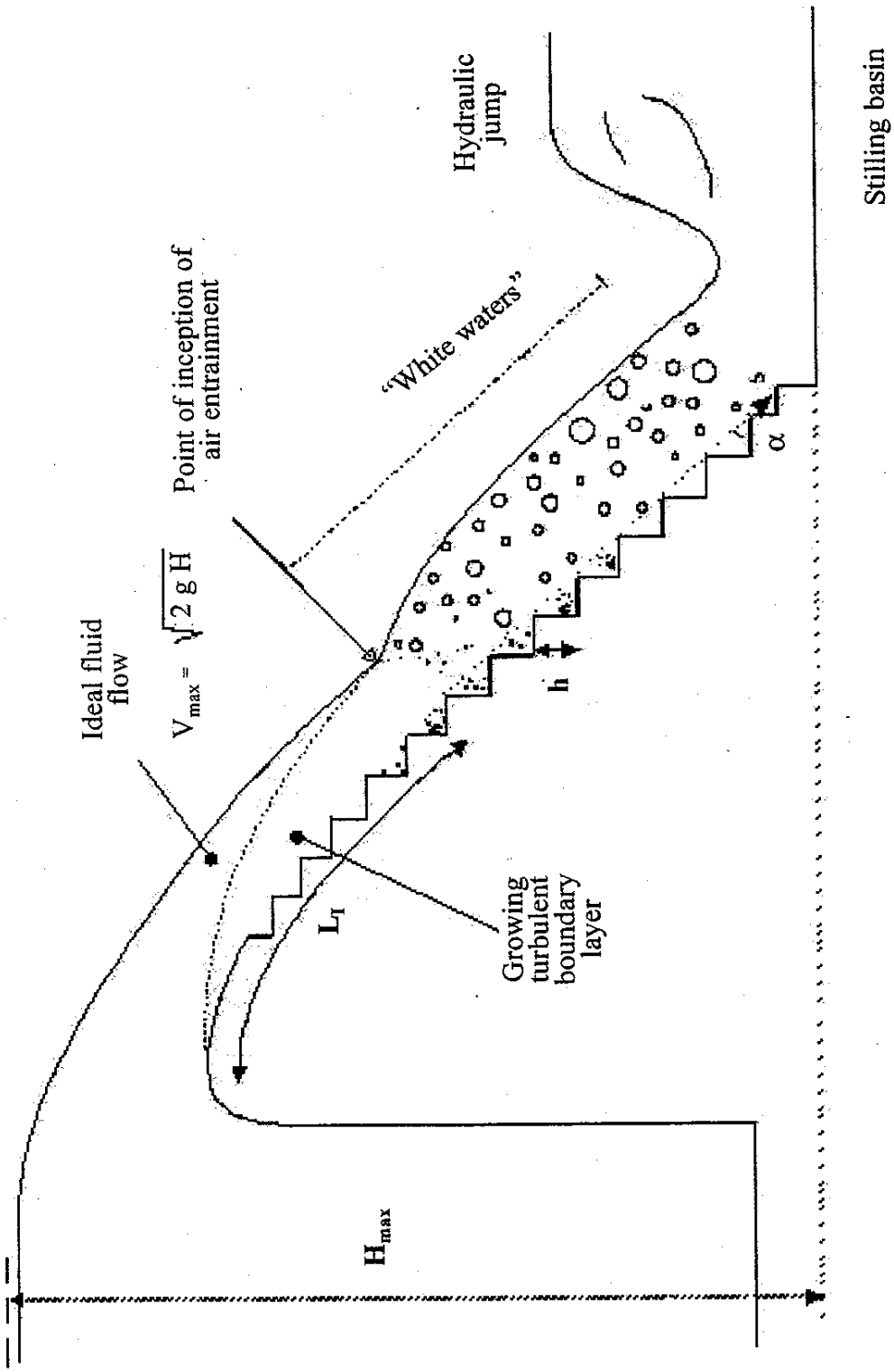

Figure 3. Basic flow regimes above a stepped chute
(c) Skimming flow regime with stable cavity recirculation

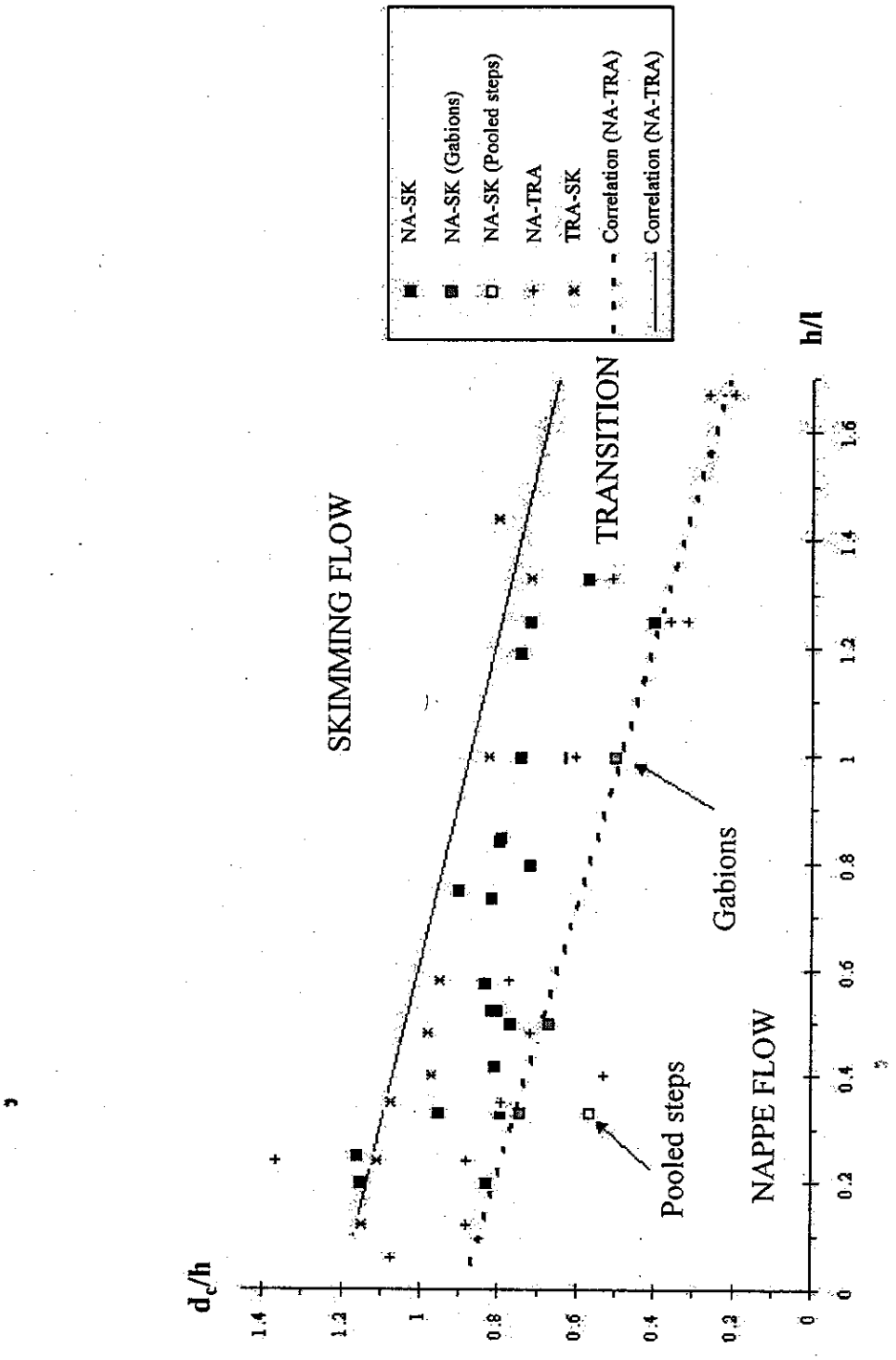

Figure 4. Flow conditions for the transition from nappe to skimming flow. Summary of experimental data (**Appendix I**)

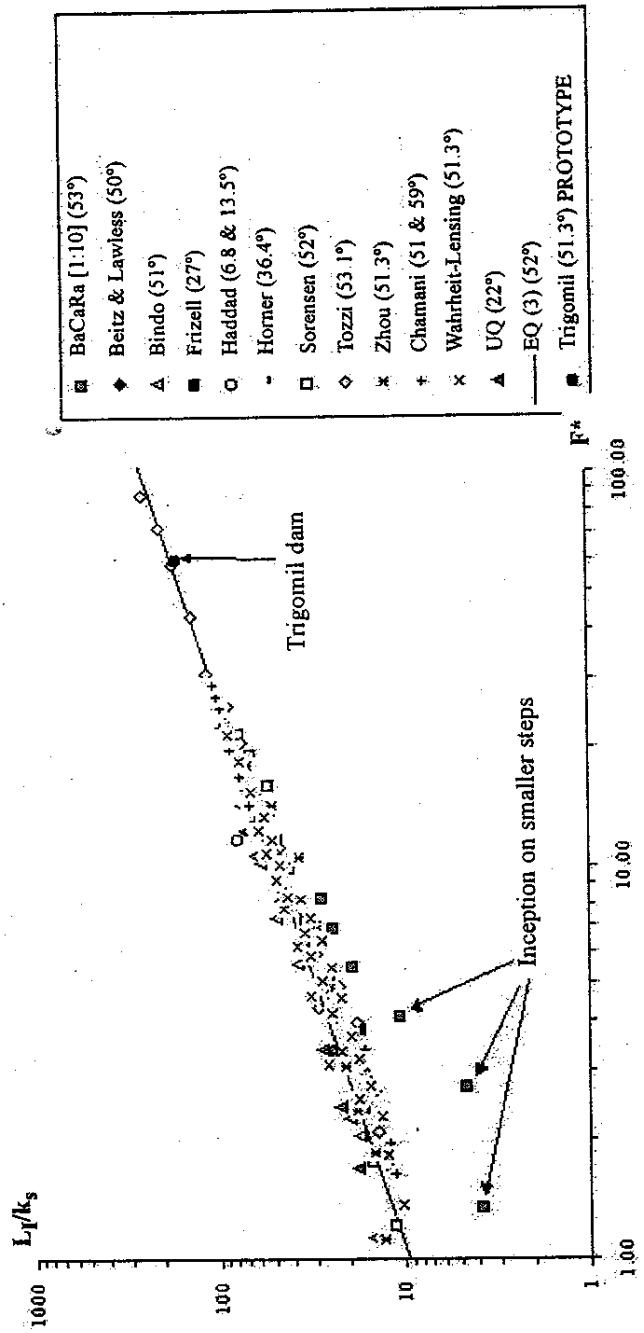

Model data: BaCaRa [1], Beitz and Lawless [3], Bindo *et al* [4], Frizell and Mefford [21], Haddad [22], Horner [24], Sorensen [36], Tozzi [38]. Present study, Wahrheit-Lensing [41], Zhou [44] - Prototype data: Trigomal dam (Sanchez-Bribiesca and Gonzalez-Villareal [34]), Brushes Clough dam (Baker [2])

Figure 5. Dimensionless distance to the inception point of air entrainment: $L_I/(h^*cos\alpha)$ as a function of $F^* = q_w/\sqrt{g^*sin\alpha^*(h^*cos\alpha)^3}$

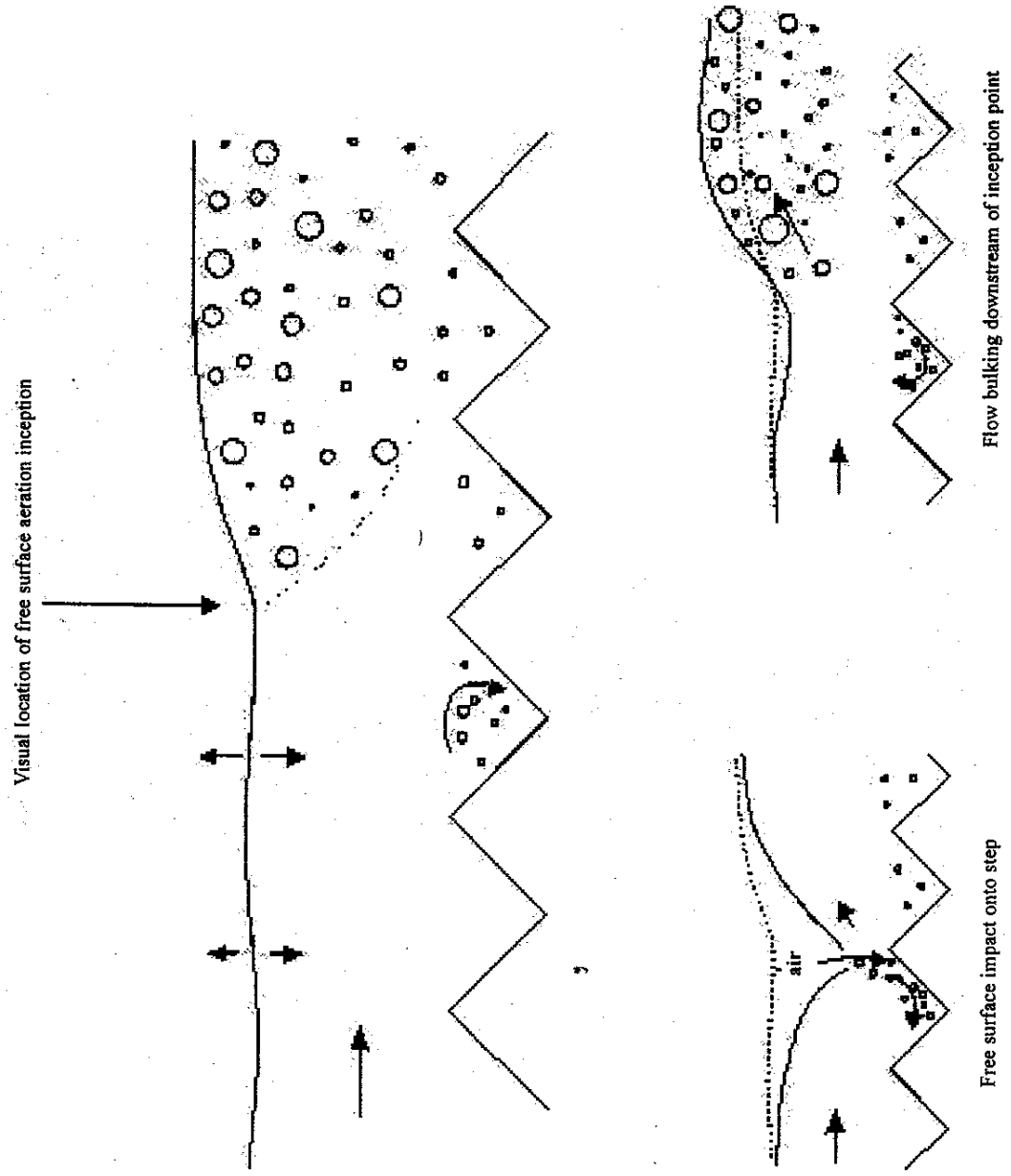

Figure 6. Rapidly varied flow region at the inception point of free surface aeration (a) Flow mechanisms next to the inception point

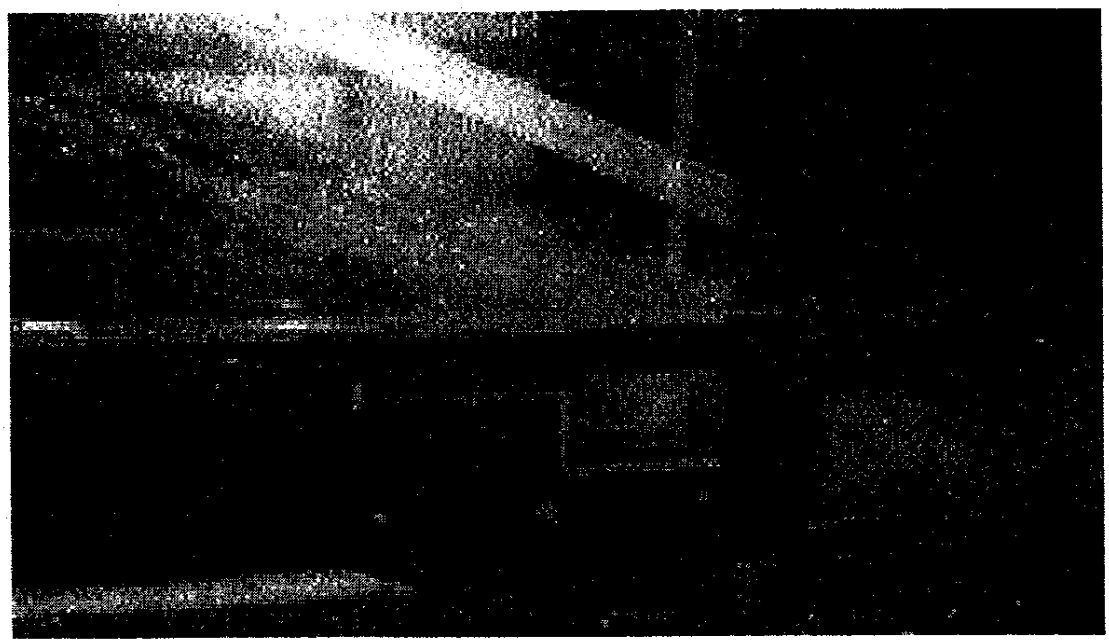

Figure 6. Rapidly varied flow region at the inception point of free surface aeration. (b) Experiment at the University of Queensland: $\alpha = 22°$, $h = 0.1$m, $W = 1$m, $d_c/h = 1.23$ – Flow from top left to bottom right. (Note the step cavity aeration upstream of free surface aeration location)

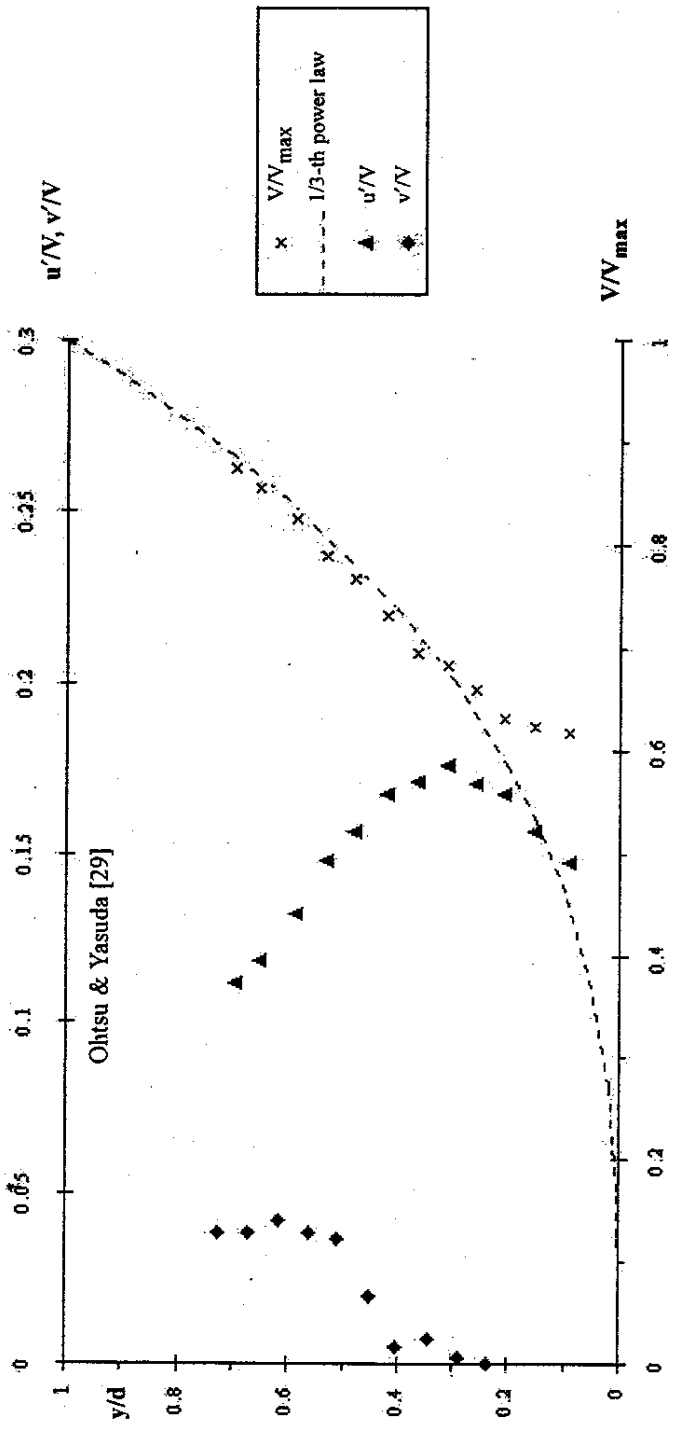

Figure 6. Rapidly varied flow region at the inception point of free surface aeration. (c) Velocity and velocity fluctuation distributions at the point of inception (Ohtsu & Yasuda [29] - $\alpha = 19°$, h = 0.05m, qw = 0.089m²/sec – Measurements at the step edge (Step 7)

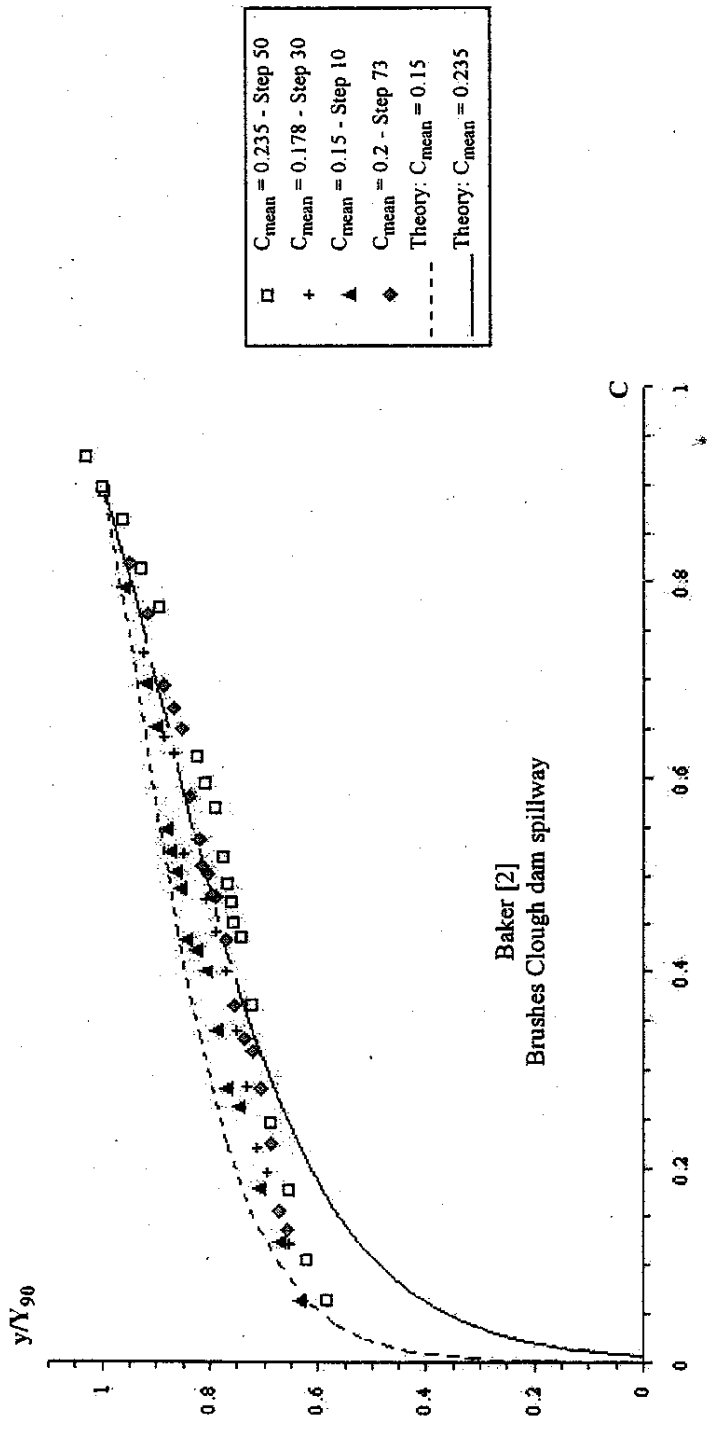

Figure 7. Void fraction distributions in stepped chute flows: comparison with Equation 6. (a) Prototype data (Baker [2])

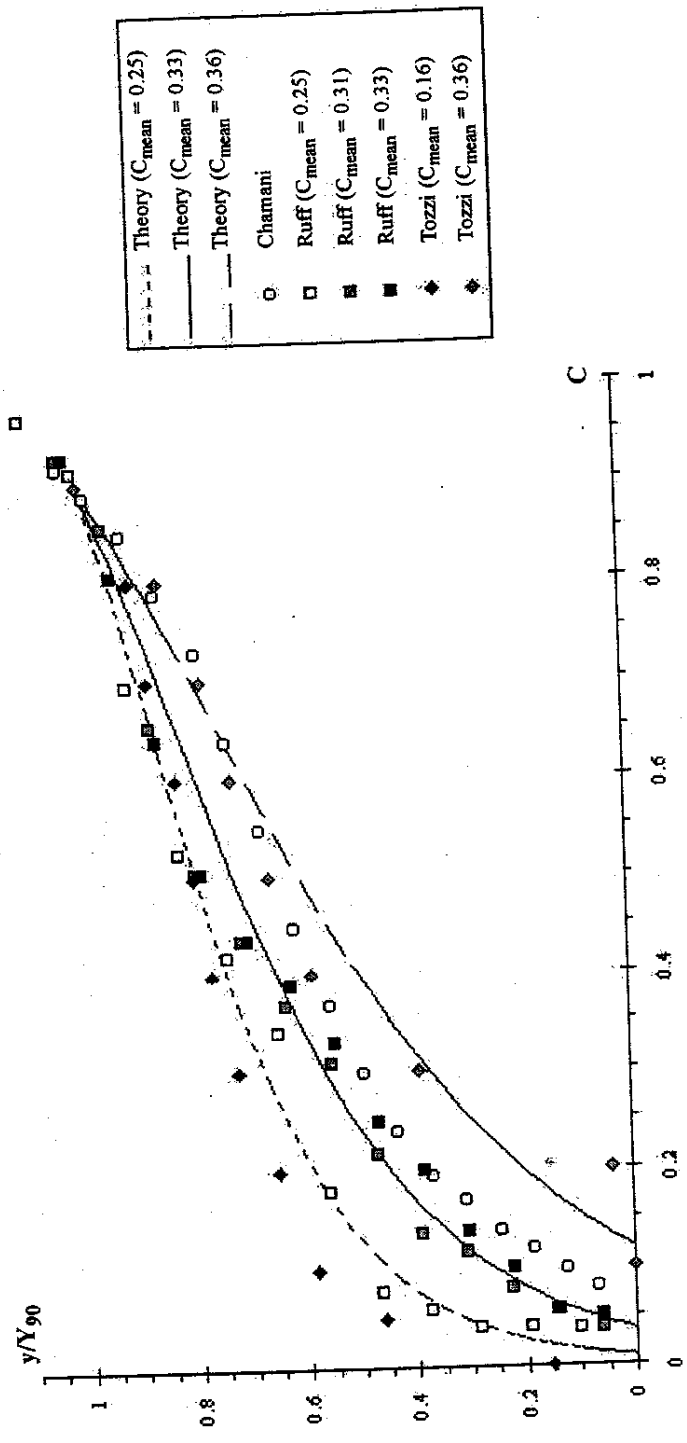

Figure 7. Void fraction distributions in stepped chute flows: comparison with Equation 6. (b) **Model data:** Ruff & Frizell [33], Tozzi *et al* [39], Chamani & Rajaratnam [9].

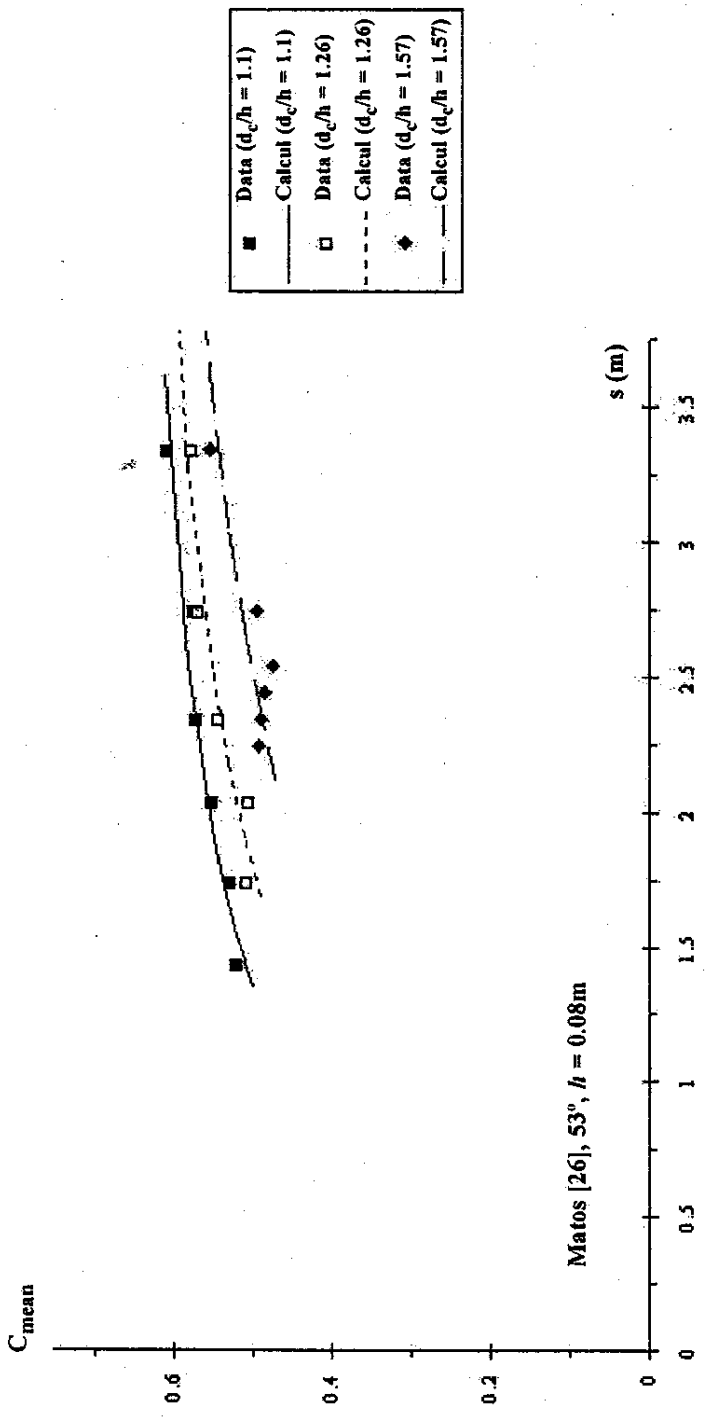

Figure 8. Self aerated flows on stepped chute: comparison between computations (Equation 8) and experimental data: $\alpha = 53.1°$, $h = 0.08$m, $u_r = 0.4$m/sec, Matos [26]

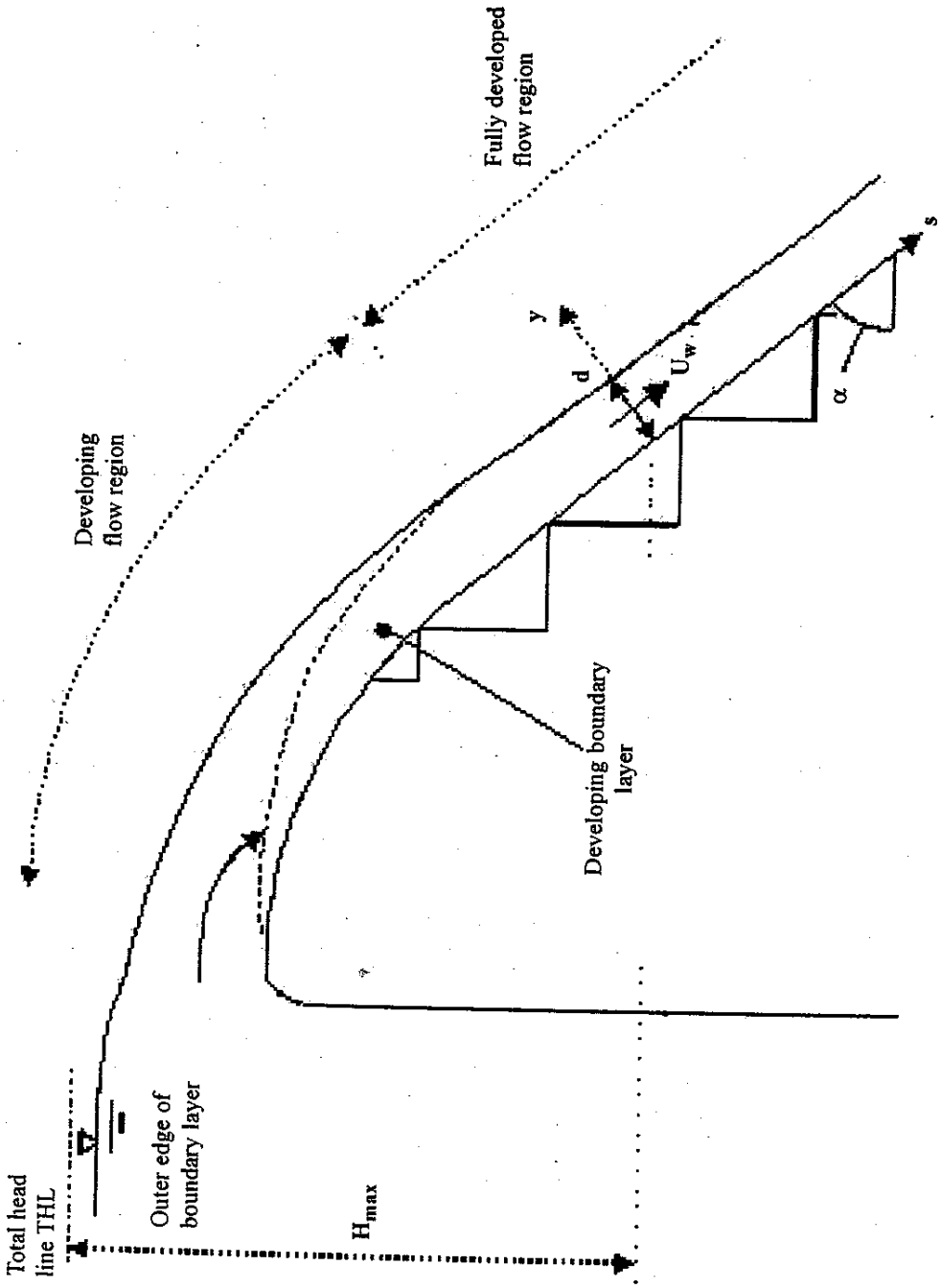

Figure 9. Residual flow velocity at the downstream end of the chute
(a) Definition sketch

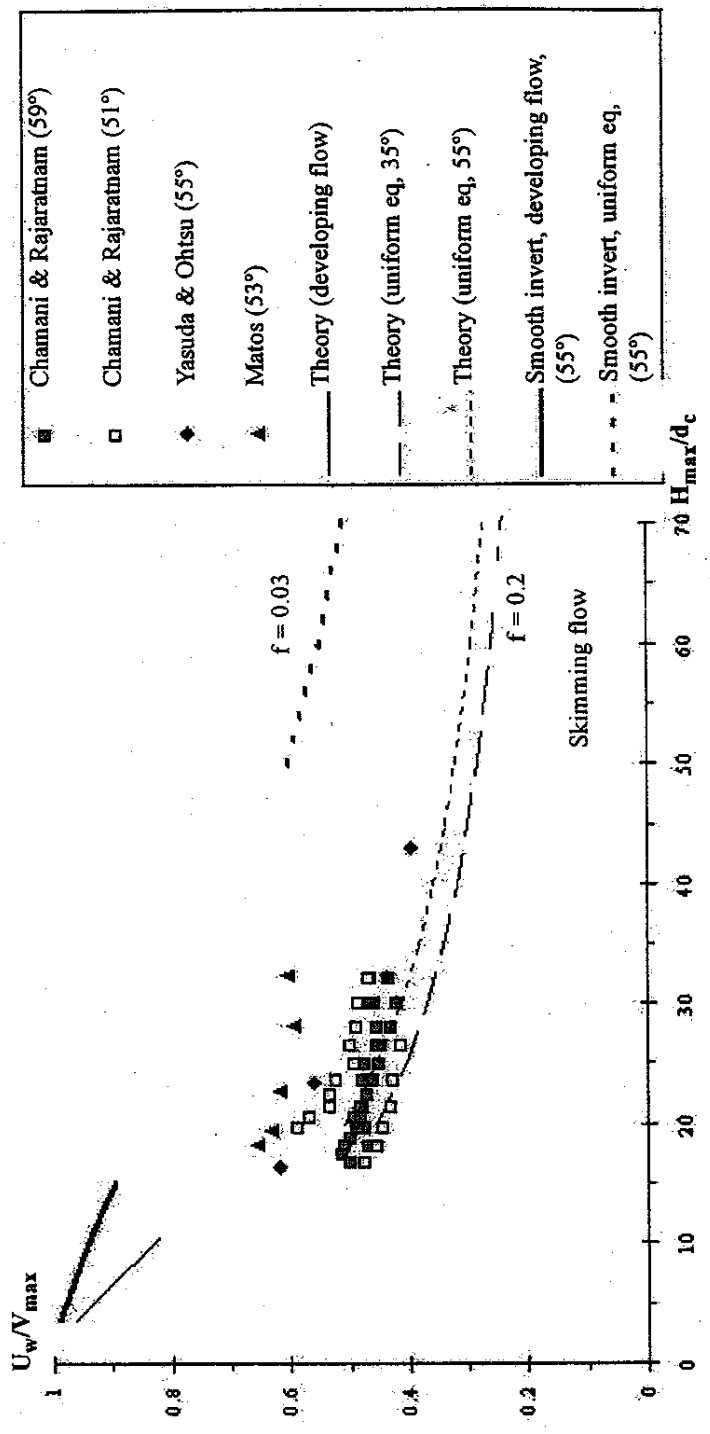

Figure 9. Residual flow velocity at the downstream end of the chute
(b) **Data**: Chamani & Rajaratnam [9], Yasuda & Ohtsu [43], Matos [26]